



Enhanced thermoelectric properties of Cu_3SbSe_4 by germanium doping

Chia-Hsiang Chang^{a,b}, Cheng-Lung Chen^{a,*}, Wan-Ting Chiu^a, Yang-Yuan Chen^{a,b,**}



^a Institute of Physics, Academia Sinica, Taipei 11529, Taiwan

^b Graduate Institute of Applied Physics, National Chengchi University, Taipei 116, Taiwan

ARTICLE INFO

Keywords:

Thermoelectric materials
Semiconductors
Sintering
Phonon
Germanium doping

ABSTRACT

Ge doped Cu_3SbSe_4 semiconductors with Cu deficiencies were synthesized by melting and spark plasma sintering for the investigation of their thermoelectric transport properties. Ge atoms can successfully substitute Sb lattice sites, and result in lattice shrinkage with increasing Ge content. Doping with Ge not only improves the electrical conductivity but also optimizes the power factor of $\text{Cu}_{2.95}(\text{Sb}_{1-x}\text{Ge}_x)\text{Se}_4$. Ge doped specimens also reveal a competition between alloying effects and increased carrier thermal conductivity. The zT enhancement of Ge doped alloys is mainly ascribed to the enhanced power factor and the reduced lattice thermal conductivity. As a result, $\text{Cu}_{2.95}(\text{Sb}_{0.96}\text{Ge}_{0.04})\text{Se}_4$ reaches a maximum zT of 0.7 at 640 K, showing an approximately 35% enhancement over the pristine $\text{Cu}_{2.95}\text{SbSe}_4$.

1. Introduction

Using thermoelectric materials to convert waste heat into electricity offers an alternative way in improving fuel economy. The thermoelectric performance of materials is evaluated by the figure of merit, $zT = \sigma S^2 T / \kappa$, where S , T , σ and κ are, Seebeck coefficient, absolute temperature, electrical and thermal conductivity, respectively [1]. The product (σS^2) is known as a power factor. The enhanced zT can be achieved by maximizing the power factor and/or minimizing the thermal conductivity.

Recently copper based chalcogenide semiconductors have emerged as potential thermoelectric materials because of their excellent electrical transport properties and relatively low thermal conductivity [2–5]. Cu_3SbSe_4 crystallizes in the Famatinite structure and belongs to this class of materials [6]. Previous works have mentioned the optimization of carrier concentration through Cu deficiencies or partial substitutions on Sb or Se sites by other elements [7]. Cu vacancies can contribute the extra carriers; however, carrier concentration will not continuously increase with Cu deficiency increment. Optimized carrier concentration for maximizing zT in Cu_3SbSe_4 might be achieved by doping some potential dopants in Sb or Se sites. Ge has been suggested a promising dopant in this material system, but only few literatures are available [7]. Herein, we reported the enhanced zT from the doped $\text{Cu}_{2.95}(\text{Sb}_{1-x}\text{Ge}_x)\text{Se}_4$, and discussed the optimization of electrical- and thermal properties in this material system. The maximum zT value of 0.7 at 640 K was achieved for $\text{Cu}_{2.95}(\text{Sb}_{0.96}\text{Ge}_{0.04})\text{Se}_4$ specimen.

2. Material and methods

Elements Cu, Sb, Se, and Ge, all of purity of 99.999% were used for synthesizing samples with nominal compositions $\text{Cu}_{2.95}(\text{Sb}_{1-x}\text{Ge}_x)\text{Se}_4$ ($x=0, 0.01, 0.03, 0.04, \text{ and } 0.06$). The weighted elements were melted at 1123 K for several hours to achieve well-mixing, and followed a water quench in room temperature. The obtained ingot was annealed at 653 K for 40 h. The products were ground to powders, and then pressed using spark plasma sintering (SPS-515S, SPS SYNTEX INC) at 573 K, 50 MPa under vacuum for several minutes. The structure and chemical composition are examined by powder x-ray diffraction (XRD, PANalytical X'Pert Pro) and x-ray fluorescence (XRF, Rigaku). The microstructures of samples were investigated by scanning electron microscopy (SEM, JXA-8200, JEOL). The measurements of Seebeck coefficient and electrical conductivity were carried out by a commercial system (ZEM-3, ULVAC-RIKO). The thermal conductivity values were determined using the equation $\kappa = D\lambda C_p$, where D , λ , and C_p are the mass density, thermal diffusivity, and heat capacity, respectively. The density was calculated using the Archimedes method. The thermal diffusivity was measured by the laser flash method (LFA-457, NETZSCH), and the heat capacity was measured using a differential scanning calorimeter (DSC-Q100, TA). The Hall measurements were carried out in a magnetic field up to ± 2 T by a Physical Property Measurement System (PPMS, Quantum Design).

* Corresponding author.

** Corresponding author at: Institute of Physics, Academia Sinica, Taipei 11529, Taiwan.

E-mail addresses: aabbs@gate.sinica.edu.tw (C.-L. Chen), cheny2@gate.sinica.edu.tw (Y.-Y. Chen).

3. Results and discussion

XRD and XRF spectroscopy were utilized to examine the material structures and chemical composition. All the diffraction patterns were indexed to the Cu_3SbSe_4 phase with tetragonal structure (PDF #85-0003), indicating no impurity phases were observed within the detection limitation (Fig. 1a). The lattice parameters decrease gradually with increasing Ge doping levels, and the consequence can be attributed to the smaller size of Ge ion (Fig. 1b). The result confirms the substitution of Ge for the Sb site. The XRF analysis revealed that the amounts of Cu, Sb, Ge and Se were extremely close to their nominal compositions and the distribution of the elements in the alloy was nearly completely homogeneous. The average grain size of these samples is approximately 1–20 μm (Fig. 1c).

Fig. 2a shows the temperature dependence of Seebeck coefficients of $\text{Cu}_{2.95}\text{Sb}_{1-x}\text{Ge}_x\text{Se}_4$ with different Ge contents. All the samples exhibited *p*-type character. The gradual decrease in Seebeck coefficient with increasing Ge content is consistent with the increase of Hall carrier concentration (Table 1 and Fig. 2d). In contrast to the undoped sample, the electrical resistivity of Ge doped samples increases slightly with temperature, exhibiting a typical degenerate semiconductor behavior (Fig. 2b). Meanwhile, a remarkable decreased electrical resistivity with increasing Ge content can be attributed to the increased carrier concentration as well. The measured electrical conductivity, Hall carrier concentration and mobility for all samples at 300 K are summarized in Table 1. The power factors are sensitive to both Ge content and temperature, and are very crucial to the *zT* enhancement (Fig. 2c). The maximum power factor of 1330 $\mu\text{W m}^{-1} \text{K}^{-2}$ at 640 K was obtained for $x=0.04$ specimen. Fig. 2d shows the carrier concentration dependence of the Seebeck coefficient (the Pisarenko relation) at 300 K. We found that the simple single parabolic band model with

acoustic phonon scattering assumption can well explain the change of transport properties of Ge doped specimens, and suggests a density-of-state effective mass m^* of 1.5 m_e . The detailed mathematic equations for describing the relationship between Seebeck coefficient and Hall carrier concentration can be found in the literature [8].

The total thermal conductivities as a function of temperature for $\text{Cu}_{2.95}(\text{Sb}_{1-x}\text{Ge}_x)\text{Se}_4$ ($0 \leq x \leq 0.06$) samples are shown in Fig. 3a. For the undoped $\text{Cu}_{2.95}\text{SbSe}_4$, the thermal conductivity is found to be 2.98 $\text{W m}^{-1} \text{K}^{-1}$ at 300 K and decreases with temperature to 1.15 $\text{W m}^{-1} \text{K}^{-1}$ at 640 K. The total thermal conductivities κ_{tot} of Ge doped specimens did not exhibit an obvious change with Ge doping. The result is ascribed to a competition on thermal conductivity resulting from alloying effects and increasing carriers. Generally, the κ_{tot} is a summation of the lattice contribution κ_{ph} and the carrier contribution κ_{car} . The κ_{car} can be calculated through the Wiedemann–Franz law: $\kappa_{car} = L\sigma T$, where L , σ and T are Lorenz number, electrical conductivity and absolute temperature, respectively [9]. Because $\text{Cu}_{2.95}(\text{Sb}_{1-x}\text{Ge}_x)\text{Se}_4$ samples belong to degenerated semiconductors, more reliable Lorenz numbers a determined according to the reduced Fermi energy and scattering parameter [10]. The plots of κ_{car} and κ_{ph} versus temperature for all samples are shown in Fig. 3b,c. The κ_{car} increases with increasing Ge content, however, κ_{ph} shows an opposite trend owing to the enhanced alloy scattering effect. The experimental results of κ_{ph} were also analyzed with the Debye–Callaway model, in which the calculated phonon thermal conductivity is the sum of one longitudinal (κ_{LA}) and two transverse (κ_{TA} and $\kappa_{TA'}$) acoustic phonon branches. The detailed equation is expressed as followings [11]:

$$\kappa_{ph} = \kappa_{LA} + \kappa_{TA} + \kappa_{TA'} = \sum_i \kappa_i \quad (1)$$

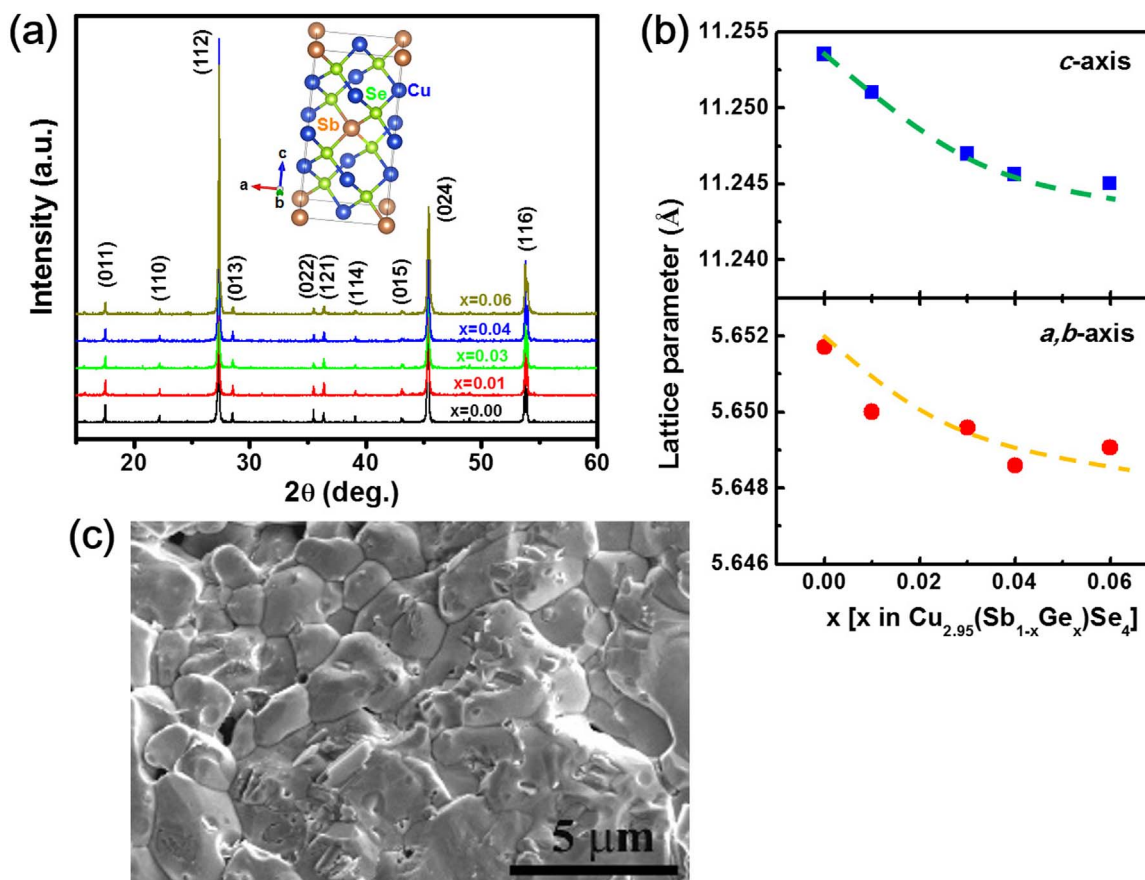


Fig. 1. (a) XRD patterns of $\text{Cu}_{2.95}(\text{Sb}_{1-x}\text{Ge}_x)\text{Se}_4$ ($0 \leq x \leq 0.06$) samples. (b) Lattice parameters as a function of x at 300 K. (c) The SEM image of fractured surface of $\text{Cu}_{2.95}\text{SbSe}_4$. The schematic crystal structure of Cu_3SbSe_4 plotted with VESTA is shown in the inset of Fig. 1(a).

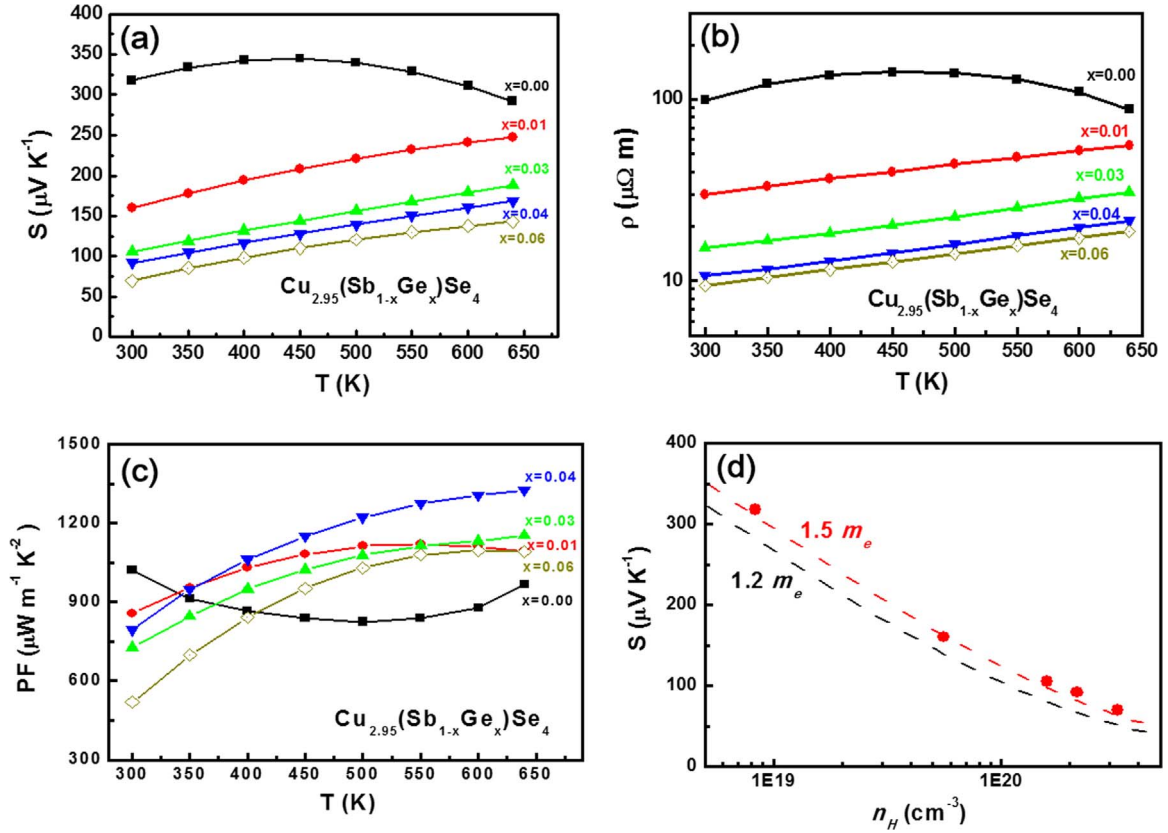


Fig. 2. Temperature dependent (a) Seebeck coefficient, (b) electrical resistivity, (c) power factor of $\text{Cu}_{2.95}(\text{Sb}_{1-x}\text{Ge}_x)\text{Se}_4$ ($0 \leq x \leq 0.06$). (d) Seebeck coefficient as a function of Hall carrier concentration at 300 K.

Table 1

Nominal composition, XRF composition, and electrical conductivity σ , Hall concentration n_H , Hall mobility μ_H , and Seebeck coefficient S at 300 K for $\text{Cu}_{2.95}(\text{Sb}_{1-x}\text{Ge}_x)\text{Se}_4$ ($0 \leq x \leq 0.06$) samples.

| Nominal composition $\text{Cu}_{2.95}(\text{Sb}_{1-x}\text{Ge}_x)\text{Se}_4$ | XRF composition | σ (S cm^{-1}) | n_H ($\times 10^{19} \text{ cm}^{-3}$) | μ_H ($\text{cm}^2 \text{ V}^{-1} \text{ s}^{-1}$) | S ($\mu\text{V K}^{-1}$) |
|---|--|---------------------------------|--|---|------------------------------|
| $x=0.00$ | $\text{Cu}_{2.95}\text{SbSe}_4$ | 97.0 | 0.8 | 75.8 | 318 |
| $x=0.01$ | $\text{Cu}_{2.95}(\text{Sb}_{0.99}\text{Ge}_{0.01})\text{Se}_{3.97}$ | 333.3 | 5.6 | 37.2 | 160 |
| $x=0.03$ | $\text{Cu}_{2.95}(\text{Sb}_{0.97}\text{Ge}_{0.03})\text{Se}_{3.97}$ | 651.2 | 15.9 | 25.6 | 105 |
| $x=0.04$ | $\text{Cu}_{2.95}(\text{Sb}_{0.96}\text{Ge}_{0.04})\text{Se}_{3.97}$ | 940.0 | 21.6 | 27.2 | 92 |
| $x=0.06$ | $\text{Cu}_{2.95}(\text{Sb}_{0.94}\text{Ge}_{0.06})\text{Se}_{3.98}$ | 1062.7 | 32.4 | 20.5 | 69 |

$$\kappa_i = \frac{1}{3} C_i T^3 \left\{ \int_0^{\Theta_i} \frac{\tau_c^i(\xi) \xi^4 e^{\xi}}{(e^{\xi}-1)^2} d\xi + \frac{\left[\int_0^{\Theta_i} \frac{\tau_c^i(\xi) \xi^4 e^{\xi}}{\tau_N^i(\xi) (e^{\xi}-1)^2} d\xi \right]^2}{\int_0^{\Theta_i} \frac{\tau_c^i(\xi) \xi^4 e^{\xi}}{\tau_N^i(\xi) (e^{\xi}-1)^2} d\xi} \right\} \quad (2)$$

where Θ_i is the longitudinal (transverse) Debye temperature, $\xi = \hbar\omega/k_B T$, and $C_i = k_B^4 / 2\pi^2 \hbar^3 v_i$, v_i is the longitudinal or transverse acoustic phonon velocity, ω is the phonon frequency, U and N are the phonon-phonon Umklapp and Normal processes, respectively. τ_c is the relaxation time, which is highly dependent on the Grüneisen parameter γ of each mode. The lattice thermal conductivity in Eq. (1) was calculated by using the parameters shown in Table S1. The above-mentioned parameters are closed to the results obtained from density functional theory phonon calculations [12]. However, the simulated curve only explained the experimental data near 300–400 K (Fig. 3c). More theoretical calculations, especially the Grüneisen parameters at $T > 400$ K, should be performed to model the thermal properties in this material system [13].

The temperature dependence of zT values for $\text{Cu}_{2.95}(\text{Sb}_{1-x}\text{Ge}_x)\text{Se}_4$ ($0 \leq x \leq 0.06$) are presented in Fig. 3d, and show a considerable increase at high temperature region. The maximum zT of 0.7 was achieved at

640 K for $\text{Cu}_{2.95}(\text{Sb}_{0.96}\text{Ge}_{0.04})\text{Se}_4$ specimen, showing an approximately 35% enhancement over the pristine $\text{Cu}_{2.95}\text{SbSe}_4$ specimen. The significant zT enhancement can be mainly attributed to the improved electrical conductivity and the reduced lattice thermal conductivity. Continuous increase in the Ge content does not further enhance zT owing to the deteriorated Seebeck coefficient and the increased total thermal conductivity. Appropriate Ge doping amount is required to optimize the carrier concentrations and the total thermal conductivity, and then reaches a maximum zT value.

4. Conclusions

In summary, Ge doping can successfully tune the carrier concentration of $\text{Cu}_{2.95}\text{SbSe}_4$ samples and achieve optimization of the power factor. The transport behavior of these alloys was analyzed with a single parabolic band model, and the density-of-state effective mass was estimated to be $1.5 m_e$. The maximum zT of 0.7 at 640 K was achieved for $\text{Cu}_{2.95}(\text{Sb}_{0.96}\text{Ge}_{0.04})\text{Se}_4$ specimen.

Acknowledgements

This work was supported by the Ministry of Science and Technology

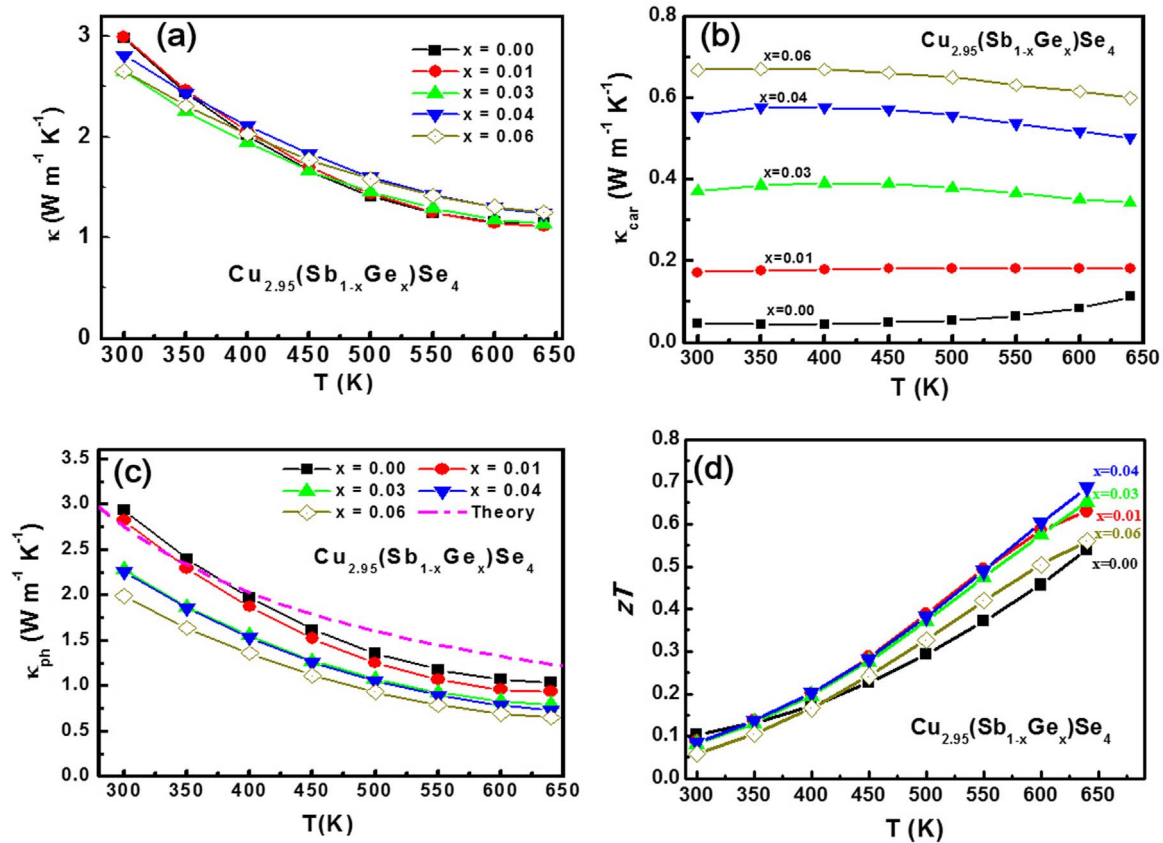


Fig. 3. Temperature dependence of (a) total thermal conductivity, (b) carrier thermal conductivity, (c) phonon thermal conductivity, and (d) zT for Ge-alloyed $\text{Cu}_{2.95}\text{SbSe}_4$.

under Grant No. NSC 103-2112-M-001-021-MY3.

Appendix A. Supplementary material

Supplementary data associated with this article can be found in the online version at <http://dx.doi.org/10.1016/j.matlet.2016.10.011>.

References

- [1] H.J. Goldsmid, CRC Handbook of Thermoelectrics, CRC Press, Florida, 1995.
- [2] F.E. Akkad, B. Mansour, T. Hendeya, Electrical and thermoelectric properties of Cu_2Se and Cu_2S , Mater. Res. Bull. 16 (1981) 535–539.
- [3] S. Ji, T. Shi, X. Qiu, J. Zhang, G. Xu, C. Chen, et al., A route to phase controllable $\text{Cu}_2\text{ZnSn}(\text{S}_{1-x}\text{Se}_x)_4$ nanocrystals with tunable energy bands, Sci. Rep. 3 (2013) 2733.
- [4] T. Plirdpring, K. Kurosaki, A. Kosuga, T. Day, S. Firdosy, V. Ravi, et al., Chalcopyrite CuGaTe_2 : a high-efficiency bulk thermoelectric material, Adv. Mater. 24 (2012) 3622–3626.
- [5] H. Liu, X. Shi, F. Xu, L. Zhang, W. Zhang, L. Chen, et al., Copper ion liquid-like thermoelectrics, Nat. Mater. 11 (2012) 422–425.
- [6] C. Yang, F. Huang, L. Wu, K. Xu, New stannite-like p-type thermoelectric material Cu_3SbSe_4 , J. Phys. D: Appl. Phys. 44 (2011) 295404.
- [7] D.T. Do, S.D. Mahanti, Theoretical study of defects Cu_3SbSe_4 : search for optimum dopants for enhancing thermoelectric properties, J. Alloy. Compd. 625 (2015) 346–354.
- [8] Y. Pei, A.D. LaLonde, H. Wang, G.J. Snyder, Low effective mass leading to high thermoelectric performance, Energy Environ. Sci. 5 (2012) 7963–7969.
- [9] H.S. Kim, Z.M. Gibbs, Y. Tang, H. Wang, G.J. Snyder, Characterization of Lorenz number with Seebeck coefficient measurement, APL Mater. 3 (2015) 041506.
- [10] D.M. Rowe, C.M. Bhandari, Modern Thermoelectrics, Prentice Hall, New Jersey, 1983.
- [11] Y. Zhang, E. Skoug, J. Cain, V. Ozoliņš, D. Morelli, C. Wolverton, First-principles description of anomalously low lattice thermal conductivity in thermoelectric Cu-Sb-Se ternary semiconductors, Phys. Rev. B 85 (2012) 054306.
- [12] Y. Zhang, E. Skoug, J. Cain, V. Ozoliņš, D. Morelli, C. Wolverton, First-principles description of anomalously low lattice thermal conductivity in thermoelectric Cu-Sb-Se ternary semiconductors, Phys. Rev. B 85 (2012) 054306.
- [13] W. Qiu, L. Wu, X. Ke, J. Yang, W. Zhang, Diverse lattice dynamics in ternary Cu-Sb-Se compounds, Sci. Rep. 5 (2015) 13643.